# Tissue Expression of Inducible Nitric Oxide Synthase Is Closely Associated with Resistance to *Leishmania major*

By Steffen Stenger, Heike Thüring, Martin Röllinghoff, and Christian Bogdan

*From the Institute of Clinical Microbiology and Immunology, University of Erlangen, D-91054 Erlangen, Germany*

## Summary

Previous studies with inhibitors of inducible nitric oxide synthase (iNOS) suggested that high-output production of nitric oxide (NO) is an important antimicrobial effector pathway in vitro and in vivo. Here, we investigated the tissue expression of iNOS in mice after infection with *Leishmania major*. Immunohistochemical staining with an iNOS-specific antiserum revealed that in the cutaneous lesion and draining lymph nodes (LN) of clinically resistant mice (C57BL/6), iNOS protein is found earlier during infection and in significantly higher amounts than in the nonhealing BALB/c strain. Similar differences were seen on the mRNA level as quantitated by competitive polymerase chain reaction. Anti-CD4 treatment of BALB/c mice not only induced resistance to disease, but also restored the expression of iNOS in the tissue. In situ, few or no parasites were found in those regions of the skin lesion and the draining LN which were highly positive for iNOS. By double labeling experiments, macrophages were identified as iNOS expressing cells in vivo. In the lesions of BALB/c mice, cells staining positively for transforming growth factor β (TGF-β), a potent inhibitor of iNOS in vitro, were strikingly more prominent than in C57BL/6, whereas no such difference was found for interleukin 4 or interferon γ (IFN-γ). In vitro, production of NO was approximately threefold higher in C57BL/6 than in BALB/c macrophages after stimulation with IFN-γ. We conclude that the pronounced expression of iNOS in resistant mice is an important mechanism for the elimination of *Leishmania* in vivo. The relative lack of iNOS in susceptible mice might be a consequence of macrophage deactivation by TGF-β and reduced responsiveness to IFN-γ.

C ytokine-induced synthesis of nitric oxide (NO)[1] from L-arginine appears to be characteristic for mammalian organisms and was first described in murine peritoneal macrophages almost 10 yr ago (1). Since then, inducible nitric oxide synthase (iNOS), the enzyme which catalyzes the conversion of L-arginine and molecular oxygen to L-citrulline and NO, has been purified, cloned, and shown to be expressed by many other cells, e.g., fibroblasts, endothelial cells, hepatocytes, articular chondrocytes, cardiac myocytes, and keratinocytes (2–4). Depending on the type of the producing cell, the site of release, and presumably also on the local NO concentration, the generation of NO by iNOS may lead to diverse consequences. Whereas iNOS is implicated in the

induction of hypotension and cardiovascular shock, the suppression of T lymphocyte responses and the damage of tissue during acute or chronic inflammatory reactions (for reviews see references 3 and 5), current data leave no doubt that NO also exerts a number of host-protective functions, including the destruction of tumor cells, metazoan and protozoan parasites, fungi, bacteria, and viruses (6–8). Antimicrobial activity of macrophage-derived NO and/or subsequent oxidation products is strongly suggested by three different sets of experimental evidence (6, 7). First, accumulation of nitrite as a measurement for the release of NO in cytokine-activated cell cultures parallels the killing of intracellular microbes. Conversely, parasite elimination was inhibited in the presence of N^ω^-monomethyl-L-arginine (L-NMMA), a substrate analogue for iNOS. Second, NO or NO-generating compounds were shown to exert a direct cytotoxic effect on some pathogens. Third, application of L-NMMA caused clinical exacerbation of certain infections in mice along with a reduced urinary excretion of nitrite and nitrate. So far, however, only little is known about

---

[1] *Abbreviations used in this paper:* AEC, 3-amino-9-ethylcarbazole; iNOS, inducible nitric oxide synthase; L-NMMA, N^G^-monomethyl-L-arginine; NADPH, nicotinamide adenine dinucleotide phosphate (reduced form); NO, nitric oxide; RT, reverse transcriptase.

the tissue expression, cellular distribution, and local activity of iNOS during the course of an infectious disease.

An area of research directly related to the antimicrobial role of NO is the analysis of the induction as well as suppression of macrophage iNOS by cytokines (9, 10). In vitro, IFN-γ appears to be the dominant iNOS-inducing agent in macrophages, and synergizes with, but does not require the presence of additional host-derived factors or microbial products (11). Similarly, TGF-β is unique within the group of cytokines shown to inhibit iNOS activity in macrophages. Compared to IL-4 (12, 13), IL-10 (14, 15), and IL-13 (16) (Bogdan, C., H. Thüring, S. Stenger, and M. Röllinghoff, manuscript in preparation), TGF-β is a markedly more potent inhibitor of the induction of iNOS when added simultaneously with the activator IFN-γ (17, 18). In addition, TGF-β, but none of the other cytokines, is able to deactivate macrophages in the strict sense of the word, i.e., to reduce the amount of iNOS protein and to shut down its activity in fully activated macrophages (18). The question arises whether the presence of IFN-γ and TGF-β also correlates with the up- and down-regulation of iNOS in vivo.

In this study we evaluated the tissue expression of iNOS and cytokines during infection of mice with *Leishmania major*. We chose the model of murine cutaneous leishmaniasis for our in situ analysis because previous studies suggested an antileishmanial effect of NO (19, 20). In vitro, leishmania replicate within nonactivated macrophages, whereas cytokine-stimulated macrophages restrict the growth of the parasite in a NO-dependent manner (21, 22). The immune response to *L. major* differs markedly in genetically resistant (e.g., C57BL/6) and susceptible mice (e.g., BALB/c) and leads to the expansion of Th1 or Th2 lymphocytes, respectively, followed by a divergent cytokine expression pattern in vivo (23-28). Treatment with neutralizing anticytokine antibodies and the transfer of *L. major*-specific Th1 or Th2 cell lines suggest that the Th1 cytokine IFN-γ confers protection, whereas the Th2 cytokine IL-4 (and IL-10) mediates fatal disease (29-31). However, little is known how these cytokines actually act in vivo (32, 33). The expression of TGF-β has not been compared in healing vs. nonhealing *L. major*-infected mice, but TGF-β was shown to aggravate infections with other *Leishmania* species (34).

Based on these observations, the *L. major* model appears to be particularly promising in order to address the following questions: (*a*) Do mice which clinically resolve the infection exhibit higher levels of iNOS in the skin lesion and the lymphoid tissue as compared to susceptible mice? (*b*) Are macrophages, which require NO to kill leishmania in vitro, also an important source of iNOS in vivo? (*c*) Does resistance or susceptibility to disease correlate with the appearance of activating (IFN-γ) or deactivating (TGF-β, IL-4, and IL-10) cytokines in the tissue leading to a differential regulation of iNOS in situ?

## Materials and Methods

*Animals, Parasites, In Vivo Infection, and Treatment.* Female BALB/c and C57BL/6 mice, weighing 16–18 g, were purchased from Charles River Breeding Laboratories (Sulzfeld, Germany), housed in our own facilities, and used at 6–8 wk of age. Origin, in vivo passage, and in vitro propagation of the *L. major* isolate were reported in detail elsewhere (35, 36). Infections were performed with thoroughly washed stationary-phase *L. major* promastigotes after two to four in vitro subcultures. In some experiments, stationary-phase promastigotes were enriched for metacyclic parasites by peanut-lectin agglutination of the noninfective procyclic organisms (37), but this did not lead to significant differences in the lesion development or the expression of iNOS. Groups of three mice per experimental time point were inoculated intradermally at the base of the tail or into the hind footpad with 3–5 × 10⁶ parasites in 25 μl of PBS. In three experiments, mice were infected bilaterally so that the tissue from one animal could be processed for both immunohistological and PCR analysis (see below). For induction of resistance, BALB/c mice were injected with 250 μg i.p. of monoclonal anti-CD4 Ab YTS 191.1 (ammonium sulphate–precipitated ascites fluid in PBS) on day −2, −1, and 0 relative to the infection, whereas control animals received PBS.

*Monitoring of the Course of Infection.* At regular intervals after infection, the footpad swelling was measured with a metric caliper (35) or the tailbase skin lesions were scored according to the following system: 0 = no visible lesion or healed scar, 1 = swelling ≤5 mm in diameter, 2 = swelling >5 mm in diameter, 3 = open lesion, ≤5 mm in diameter, and 4 = open lesion >5 mm in diameter. In addition to the clinical course of disease, we also monitored the parasite burden in the tissue of infected mice by a modified limiting dilution procedure as published earlier (35).

*Cytokines, Primary Abs, and other Reagents.* Recombinant murine IFN-γ (batch M3RD48; protein concentration 1.0 mg/ml; sp act 5.2 × 10⁶ U/mg; LPS content <10 pg/ml) was a gift from Dr. G. Adolf (Ernst Boehringer Institut für Arzneimittelforschung, Vienna, Austria). Recombinant human IL-1β (protein concentration 0.98 mg/ml; sp act 1.2 × 10⁷ U/mg; LPS content <52 pg/ml) was kindly provided by Amgen (Thousand Oaks, CA). Smooth strain LPS, prepared by phenol extraction from *Escherichia coli* 0111:B4, and Con A (lot 12H9408; LPS content 0.2 ng/ml at 10 mg/ml) were obtained from Sigma Chemie (Deisenhofen, Germany).

A polyclonal anti-*L. major* antiserum was generated in rabbits (36) and generously supplied by Dr. H. Moll (Zentrum für Infektionsforschung, Würzburg, Germany). Rabbit anti–mouse iNOS IgG antibodies were raised against iNOS purified from the RAW 264.7 cell line or against an octapeptide derived from the COOH terminus of murine iNOS and were kindly provided by Drs. Q.-w. Xie, C. Nathan (Cornell University Medical College, New York) (38) and Drs. J. R. Weidner and R. A. Mumford (Merck Research Laboratories, Rahway, NJ), respectively. For the immunohistological detection of TGF-β, we used both panspecific rabbit anti-TGF-β IgG which neutralizes TGF-β1, TGF-β2, TGF-β3, and TGF-β5 (AB-100-NA, lot BO 033041; R&D Systems, Inc., Minneapolis, MN), and a protein A–purified rabbit anti-TGF-β1 antiserum which was generated against a peptide corresponding to amino acids 1-30 of TGF-β1 (generously provided by Drs. Kathy Flanders and Mike Sporn, National Cancer Institute, Bethesda, MD). The rat mAbs BM8 (IgG2a; pan-tissue macrophage), M1-70 (IgG2b; Mac-1 [CD11b]), C1.A.3-1 (IgG2b; F4/80 antigen on monocytes and tissue macrophages), MOMA-2 (IgG2b; monocytes and macrophages), RB6-8C5 (IgG2b; GR-1 antigen on granulocytes), XMG1.2 (IgG1; anti-IFN-γ), BVD4-1D11 (IgG2b; anti-IL-4), and JES5-2A5 (IgG1; anti-IL-10) were all purchased from Dianova Inc. (Hamburg, Germany). The rat mAbs YTS191.1 (IgG2b; anti-CD4), YTS169.4 (IgG2b; anti-CD8), and anti-B220 were obtained from Serva Inc. (Heidelberg, Germany).

*Isolation of Cells and Tissue, Cell Separation, and Cell Culture.* For isolation of total RNA, organs from uninfected or infected mice were flash frozen in liquid nitrogen and stored at −70°C, while the contralateral tissue samples were embedded in specimen molds (cryomold®) using optimal cutting temperature (OCT) compound (Diatec, Hallstadt/Bamberg, Germany) and stored frozen for later immunohistological analysis. For quantification of the parasite load with the limiting dilution technique, single cell suspensions of LN and spleen or homogenates of the skin lesion were prepared as described (35). For tissue culture experiments, LN or spleen cells were seeded into 96-well round-bottom microdilution plates (Nunc, Wiesbaden, Germany) and restimulated in Click's RPMI 1640 (supplemented with 10% heat-inactivated selected FBS [Sigma], 2 mM glutamine, 10 mM Hepes, 13 mM NaHCO₃, 100 µg/ml penicillin, and 160 µg/ml gentamicin [all other reagents from Seromed-Biochrom, Berlin, Germany]) with IFN-γ (20 ng/ml)/LPS (20 ng/ml) or Con A (2.5 µg/ml) plus IL-1 (50 U/ml). In some experiments, T or B lymphocytes were depleted from spleen and LN suspensions by magnetic separation with a MACS column (Miltenyi Biotech, Germany) after incubation with anti-Thy 1.2 or anti-B220 Abs coupled to magnetic particles, according to the manufacturer's instructions. The purity of the resulting T (B) cell–depleted and T (B) cell–enriched population was checked by flow cytometry using a FACScan® from Becton Dickinson & Co. (Mountain View, CA). Thioglycollate-elicited peritoneal macrophages from BALB/c and C57BL/6 mice were prepared as published previously (18) and were cultured in RPMI 1640 (Seromed-Biochrom) with 5% heat-inactivated FBS (Sigma). At the concentrations used in the tissue culture experiments, the LPS content of all reagents as well as of the supplemented media was ≤ 10 pg/ml as determined with a colorimetric *Limulus* amebocyte lysate assay (Whittaker M.A. Bioproducts, Walkersville, MD).

*Determination of NO₂⁻ Accumulation in Culture Supernatants, iNOS Enzyme Assay, SDS-PAGE, and Western Blot Analysis.* For measurement of NO₂⁻ accumulation in culture supernatants, preparation of macrophage lysates, determination of iNOS enzyme activity, and detection of iNOS protein by SDS-PAGE and Western blot, we exactly followed previously published protocols (18).

*RNA Preparation and Competitive Reverse Transcriptase (RT)-PCR.* Frozen organs were homogenized in 4 M guanidiniumisothiocyanate and total RNA was extracted as described (39). cDNAs were synthesized from 1 µg total RNA using 2.5 µM poly(dT)₁₂₋₁₈, 12.5 U AMV reverse transcriptase, 0.5 mM of each dNTP, 5 mM MgCl₂, and 32 U RNAguard (all from Pharmacia, Freiburg, Germany) in a final reaction volume of 20 µl. PCR amplification of the cDNAs was carried out during 35 cycles (1 min denaturation at 95°C, 1 min annealing at 58°C, 1 min extension at 72°C) with a DNA thermal cycler (model 480; Perkin-Elmer, Weiterstadt, Germany) in 40 µl of a reaction mixture containing 10 mM Tris, pH 8.3, 50 mM KCl, 2 mM MgCl₂, 400 µM of each dNTP, 1 U Taq DNA polymerase (all from Pharmacia), and 250 nM of upstream and downstream oligonucleotide primer (Biometra, Göttingen, Germany). PCR-amplified samples were analyzed on a 1.5% agarose gel.

An exact quantification of iNOS mRNA vs. β-actin mRNA in the various tissue samples was obtained by competitive PCR as described previously (40). Initially, each cDNA was individually amplified with β-actin–specific primers in the presence of 10-fold serially diluted actin competitor of known molarity (see below) yielding similar band intensities of the control and cDNA fragment at a defined dilution of the competitor. Thereafter, twofold dilutions of the cDNA and a fixed concentration of competitor were coamplified, which led to the appearance of exactly equal band

intensities for both fragments and, thus, to a precise quantification of the cDNA relative to the competitor. Subsequently, the same two-step procedure was performed with iNOS-specific primers using an iNOS competitor of known molarity (see below). Finally, the ratio was formed between the dilutions of the iNOS and β-actin competitor required for equal band intensities of the respective cDNA and control fragments. All PCR results presented in this study were repeated two to three times independently and are solely based on the competitive PCR technique.

*Oligonucleotides and Competitor Plasmids.* The following PCR primers were used: iNOS sense 5′-TCACGCTTGGGTCTTGTT-CACT-3′ (bp position 161 → 182 of the murine macrophage iNOS sequence [38]), iNOS antisense 5′-TTGTCTCTGGGTCCTCTG-GTCA-3′ (bp position 632 → 611), β-actin sense 5′-CACCCG-CCACCAGTTCGCCA-3′ (bp position 62 → 81 of the murine β-actin sequence [41]), and β-actin antisense 5′-CAGGTCCCG-GCCAGCCAGGT-3′ (bp position 635 → 616). The specificity of the 472-bp iNOS PCR product was confirmed by Southern blot hybridization with an internal antisense oligonucleotide probe (located at bp position 436 → 403 of the iNOS sequence) following standard protocols (42). The β-actin competitor was generated by low-stringency (annealing 37°C, 5 cycles; 60°C, 30 cycles) PCR amplification of unrelated *E. coli* DNA with β-actin primers, which yielded a control fragment slightly larger in size than the β-actin cDNA (700 vs. 574 bp), but flanked by the same β-actin–specific sequences. The control fragment was cloned into the pSPT18 vector (Boehringer, Mannheim, Germany). The iNOS competitor plasmid was obtained by insertion of a 162-bp DNA fragment (isolated from a φX174 RF DNA-HincII digest [Pharmacia]) into the HincII restriction site (position 200) of the murine iNOS clone L1, which was kindly provided by Dr. Q.-w. Xie (38). Both competitor constructs were shown to compete stochiometrically with plasmids containing the unmodified β-actin or iNOS cDNA sequence.

*Immunoenzymatic Sequencing of Tissue Sections.* As published previously (43), freshly cut cryostat sections (5 µm) were thawed onto gelatine-coated slides, air-dried for 60 min, and fixed in acetone (10 min, −20°C). The remaining OCT compound was washed off with PBS/0.05% Tween 20 and nonspecific binding sites were blocked by incubation in PBS containing 0.1% BSA and 20% FCS (30 min, room temperature) before the primary Ab of rabbit or rat origin (diluted in PBS/0.1% BSA) was added (1 h, room temperature or overnight, 4°C). Subsequently, the sections were washed (three times for 10 min, with PBS/0.05% Tween 20), incubated with affinity-purified, biotin-conjugated F(ab′)₂-fragment donkey anti–rabbit IgG or mouse anti–rat IgG (Dianova) (1 h, RT), washed again, and overlayed with preformed streptavidin-biotin-peroxidase-complex (Dako, Hamburg, Germany) for 1 h at room temperature. After a final wash, the labeling was visualized with 0.2 mg/ml 3-amino-9-ethyl-carbazole (AEC; Sigma) and 0.015% H₂O₂ in acetate buffer (50 mM, pH 5.1). The development was stopped by rinsing with 50 mM Tris, pH 7.4/0.05% Tween 20. When the first-step Abs were omitted or replaced by preimmune serum or an irrelevant isotype-matched control Ab, no staining was obtained. Optimal Ab concentrations were determined in several series of pilot experiments. The sections were counterstained with hematoxylin and mounted (Aquatex; Merck, Darmstadt, Germany). For semiquantitative evaluation of tissue sections, the number of positively stained nucleated cells was determined by visual examination of ≤50 sections per organ (at least 5,000 cells counted, at a magnification of 400).

*Double Labeling of Tissue Sections.* A combination of gold-silver immunostaining and immunoenzymatic labeling was performed exactly as published previously (43) except that we used streptavidin-
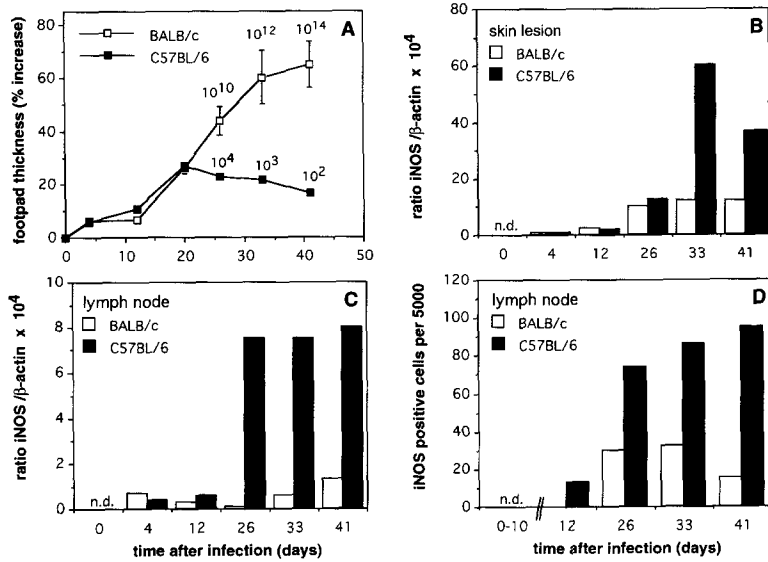
**Figure 1.** Expression of iNOS mRNA and protein after *L. major* infection. (*A*) BALB/c and C57BL/6 mice were bilaterally infected with *L. major* (3 × 10⁶) into the hind footpads and the subsequent lesion development (mean increase of footpad thickness ± SD) was monitored. Where error bars are not visible, they fall within the symbols denoting the mean. Numbers on top of the symbols represent final dilutions of footpad tissue yielding viable parasites in the limiting dilution analysis. (*B–D*) At designated time points after infection, groups of three mice were killed. iNOS mRNA and β-actin mRNA levels in the left skin lesion and popliteal LN were precisely quantitated by competitive RT-PCR of pooled RNA preparations (*B* and *C*), while the contralateral LN was processed for immunohistochemistry and the approximate number of cells staining positively for iNOS was visually determined (*D*). The data shown are representative for three similar experiments.

biotin-peroxidase complex (with AEC as substrate) instead of streptavidin-biotin-alkaline phosphatase complex for the immunoenzymatic labeling.

*NADPH Diaphorase Staining.* For detection of nicotinamide adenine dinucleotide phosphate (NADPH) diaphorase activity, acetone-fixed cryostat sections (5 μM) were incubated in 50 mM Tris buffer (pH 7.5), 0.5 mM nitroblue tetrazolium salt, 1 mM NADPH, and 0.2% Triton X-100 (37°C, 30 min) as published previously (44).

## Results

*L. major–infected Resistant Mice Express Higher Levels of iNOS mRNA and Protein in the Tissue Compared to Susceptible Mice.* In three independent experiments, organs from *L. major*–infected BALB/c and C57BL/6 mice were analyzed for the expression of iNOS at various time points during the course of disease (Fig. 1 *A*). Low levels of iNOS mRNA were already detectable by PCR in the lesions of both mouse strains 1 d after infection, but not in the skin of naive mice (data not shown). As quantitated by competitive PCR analysis (see Materials and Methods), the amount of iNOS mRNA subsequently increased by a factor of up to 100 in the lesions of resistant C57BL/6 mice, but much less so in nonhealing BALB/c mice. Thus, peak levels of iNOS mRNA were at least 6–10-fold higher in resistant animals (Fig. 1 *B*). Similar induction of iNOS mRNA occurred in the draining LN leading to high and persistent expression of iNOS in the resistant, but not in the susceptible strain (Fig. 1 *C*). Although the exact time course varied from experiment to experiment, upregulation of iNOS mRNA always correlated with the resolution of clinical disease (Fig. 1 *A* vs. Fig. 1, *B* and *C*). iNOS mRNA was also found in the spleen of infected animals, but
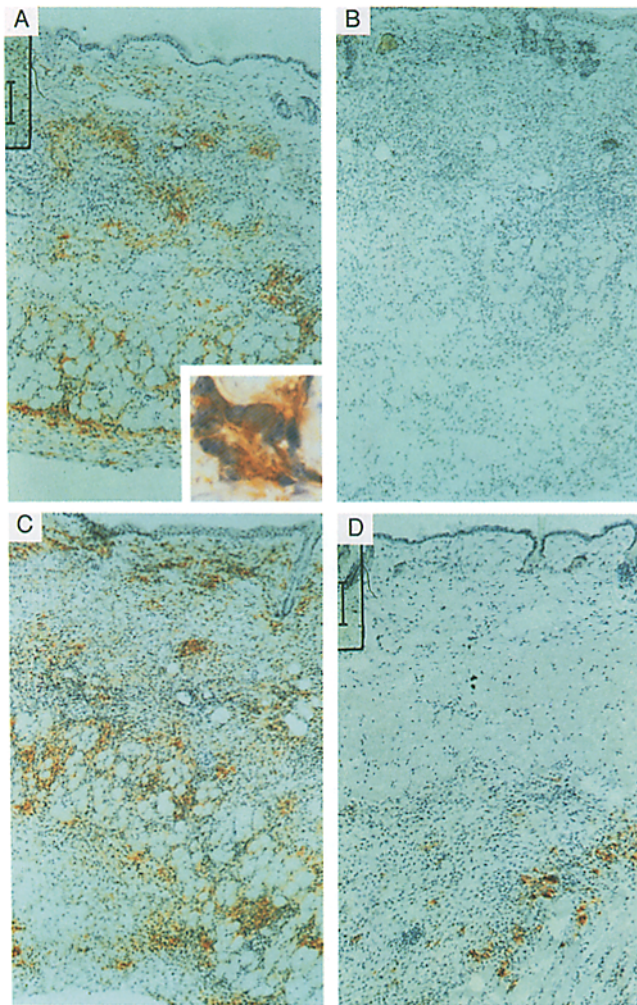


**Figure 2.** Differential expression of iNOS in the skin lesions of resistant and susceptible mice. Mice were intradermally infected with *L. major* (3 × 10⁶) at the base of the tail and the skin lesions were analyzed for the presence of iNOS by immunoperoxidase labeling of tissue sections

as described in Material and Methods. (*A*) C57BL/6, day 4 of infection. The inset shows a collection of iNOS-positive phagocytes within the subcutaneous inflammatory infiltrate. (*B*) BALB/c, day 4; (*C*) C57BL/6, day 11; (*D*) BALB/c, day 11. ×100 (bar, 100 μm) in *A–D*; ×1,000 in the inset of *A*.

the levels were at ~10-fold lower than in the regional LN (data not shown).

In parallel to the quantitation of iNOS mRNA in total organs, we carried out immunohistology in order to localize and define the expression of iNOS protein in *L. major*–infected tissue. In the cutaneous lesion, iNOS protein was undetectable at day 1 and 2 after infection in both strains of mice (data not shown), whereas it was regularly found in macrophage-rich mononuclear infiltrates of the dermis and subcutis of resistant mice from day 4 of infection onwards. Thereafter, iNOS was rapidly upregulated in resistant, but not in susceptible mice as visualized by low-power magnifications of the respective skin sections (Fig. 2, *A–D*). A similar pattern was seen in the draining LN, where iNOS was also expressed earlier (day 10–12 of infection vs. day 16–18) and to a strikingly higher extent in the resistant strain (Fig. 3, *A* and *B*). A semiquantitative analysis based on the visual enumeration of positively stained cells per 5,000 nuclei revealed that the number of iNOS-positive cells in the LN of the healer strain exceeded the values in the nonhealing mice by a factor of ≥3 at all time points of infection (Fig. 1 *D*). This approximation does not take into account our observation that, despite equal developing times, the iNOS staining was always considerably more intense in sections from C57BL/6 mice (see Fig. 3, *A* vs. *B*). The specificity of the iNOS staining could be demonstrated by several methods (data not shown): (*a*) the staining obtained was completely blocked in the presence of 0.5–1.0 μg/ml of the iNOS peptide used for generating the polyclonal rabbit antiserum; (*b*) no iNOS protein was detected in skin and LN from uninfected mice or when using the respective rabbit preimmune serum; and (*c*) in vitro, immunocytochemical iNOS staining of macro-

phages was only found after induction of iNOS mRNA and protein by IFN-γ or IFN-γ/LPS, but not in unstimulated cultures.

*Expression of iNOS in the LN Is Confined to Clusters of Macrophages.* Between day 10 and 20 of infection, iNOS was exclusively found in the paracortical or medullary region of the LN, where it colocalized with macrophages as determined by staining of consecutive tissue sections (data not shown). These macrophages were comparably well recognized by the mAbs F4/80, MOMA-2, or Mac-1 (anti-CR3). Direct demonstration of iNOS in macrophages was possible by double labeling techniques (Fig. 3, *C* and *D*). At the same stage of disease, no iNOS was detectable in the follicles of the LN, although we did find isolated MOMA-2⁺ (F4/80⁻, Mac-1⁻) macrophages in the follicles as described previously (45; data not shown). However, at later time points of infection, iNOS-positive macrophages appeared to infiltrate the follicular areas (Figs. 3 *A* and 4 *A*). Up to 50% of F4/80⁺, MOMA-2⁺, or Mac-1⁺ cells of the infected LN did not express iNOS. On the other hand, ~20% of iNOS-positive areas failed to stain with the F4/80 Ab, but were picked up by anti-CR3 (Mac-1) as well as MOMA-2 (data not shown). These results indicate that all iNOS-positive cells are located within macrophage-rich regions but by far, not all macrophages express iNOS at one time.

*Tissue Expression of iNOS Correlates with the Absence of Parasites and Colocalizes with NADPH Diaphorase Activity.* To obtain more direct evidence for the antileishmanial function of NO, we stained consecutive sections of LN with anti-iNOS and anti-*L. major* antisera. As illustrated in Fig. 4, high expression of iNOS in resistant mice was paralleled by the absence of parasites in the same region (Fig. 4, *A* and *B*), whereas
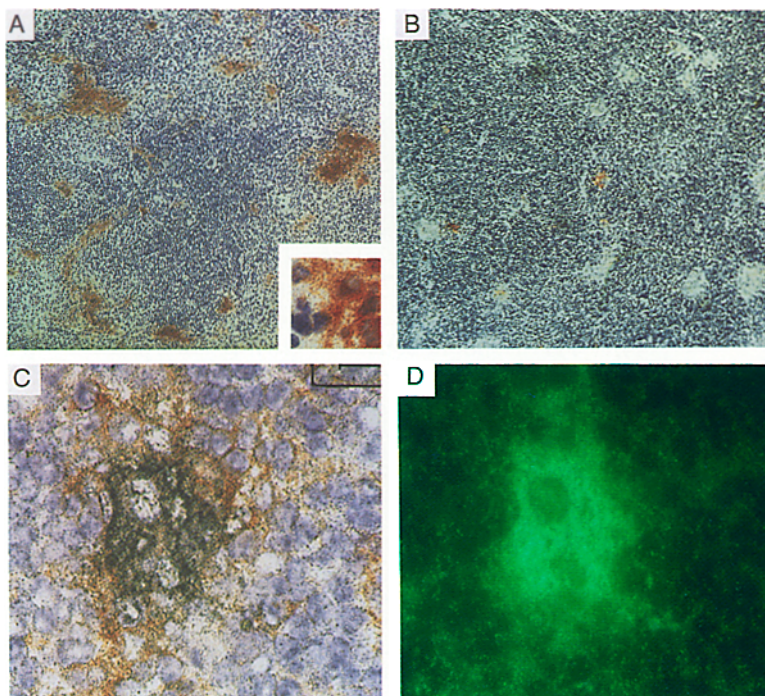


**Figure 3.** Expression of iNOS in the lymph node differs between resistant and susceptible mice and is found in macrophages. BALB/c and C57BL/6 mice were infected at the base of the tail and the inguinal LN were analyzed for the expression of iNOS and the presence of macrophages by one-color immunoperoxidase staining (*A* and *B*) or double labeling (*C* and *D*). (*A*) C57BL/6, day 26 of infection, strong anti-iNOS staining; ×100, inset ×1,000. (*B*) BALB/c, day 26, weak anti-iNOS staining, areas of necrosis, ×100. (*C* and *D*) Double staining for F4/80⁺ macrophages (immunoperoxidase labeling with substrate AEC and hematoxylin counterstaining) and iNOS (immunogold-silver staining). Some macrophages, visualized under brightfield illumination (*C*) by the brownish AEC-label, also display iNOS (dark grains, which appear light blue-greenish under epipolarization illumination [*D*]). ×1,000, bar, 10 μm.
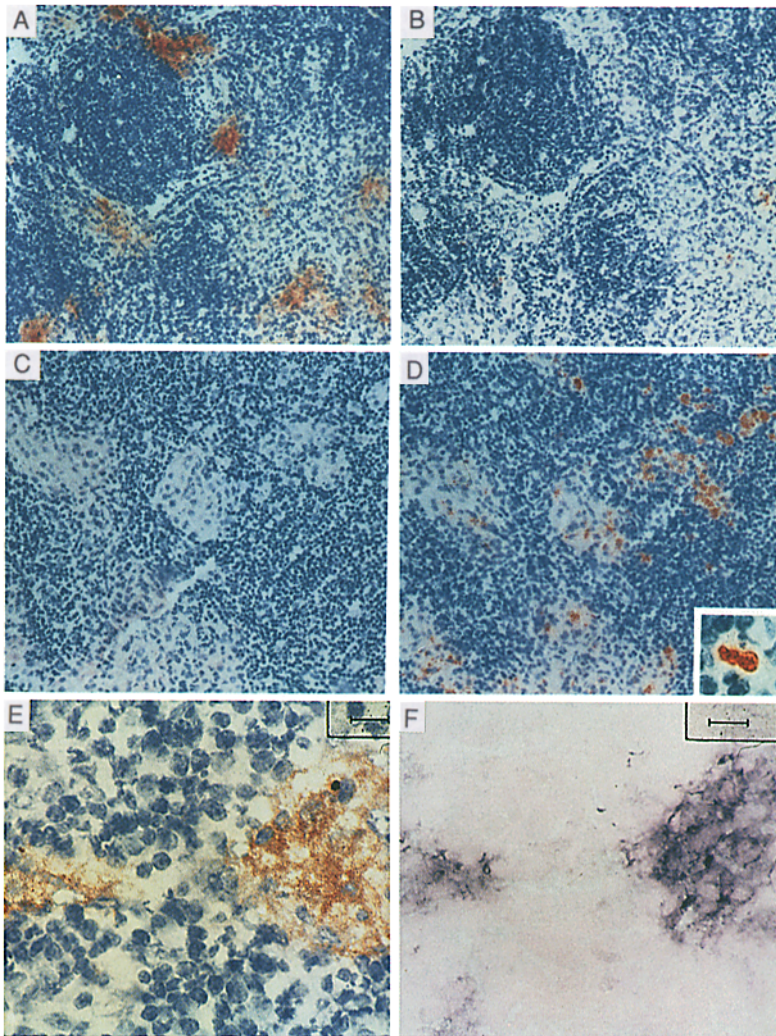
Figure 4. Expression of iNOS correlates with the absence of *L. major* parasites and the presence of NADPH diaphorase. Consecutive sections of LN from *L. major*–infected C57BL/6 or BALB/c mice were analyzed for the presence of iNOS and *L. major* by immunoperoxidase staining at day 30 of infection (*A–D*) or iNOS and NADPH diaphorase at day 26 after infection (*E* and *F*). (*A*) C57BL/6, anti-iNOS. (*B*) C57BL/6, anti-*L. major*. (*C*) BALB/c, anti-iNOS. (*D*) BALB/c, anti-*L. major*. The inset shows three *L. major* amastigotes. (*E*) C57BL/6, anti-iNOS. (*F*) C57BL/6, NADPH diaphorase. ×200 (*A–D*) or ×1,000 (inset of *A*, *E*, and *F*, bar, 10 μm).

numerous parasites were detectable in the necrotic tissue of BALB/c mice lacking the expression of iNOS (Fig. 4, *C* and *D*).

The ability of NOS to convert colorless tetrazolium salts and NADPH to purple formazan under L-arginine–free conditions has been used to localize constitutive NOS activity in neuronal tissue (44). We applied the same staining method to skin (data not shown) and LN sections of *L. major*–infected BALB/c or C57BL/6 mice and always found a perfect match between the detection of iNOS protein and NADPH diaphorase activity (Fig. 4, *E* and *F*). Areas negative for iNOS were also negative for NADPH diaphorase. Although enzymes other than iNOS are known to act as NADPH diaphorases, this result is a further indication of the presence of activated cells expressing functional iNOS.
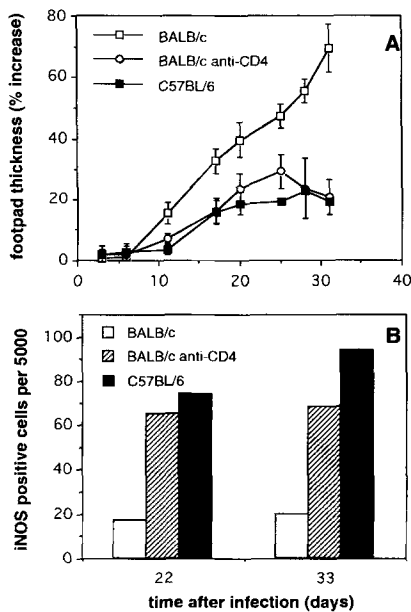


Figure 5. Anti-CD4 treatment induces clinical healing and restores expression of iNOS in *L. major*–infected BALB/c mice. C57BL/6 mice were

infected with *L. major* into the right footpad along with BALB/c mice, which were intraperitoneally injected with PBS or anti-CD4 before infection (see Materials and Methods). The clinical course of the infection was monitored (*A*). At day 22 and 33 of infection, three mice of each group were killed, tissue sections of the popliteal LN were labeled with anti-iNOS/immunoperoxidase and the approximate number of iNOS⁺ cells (*B*) was visually determined. One of two comparable experiments.
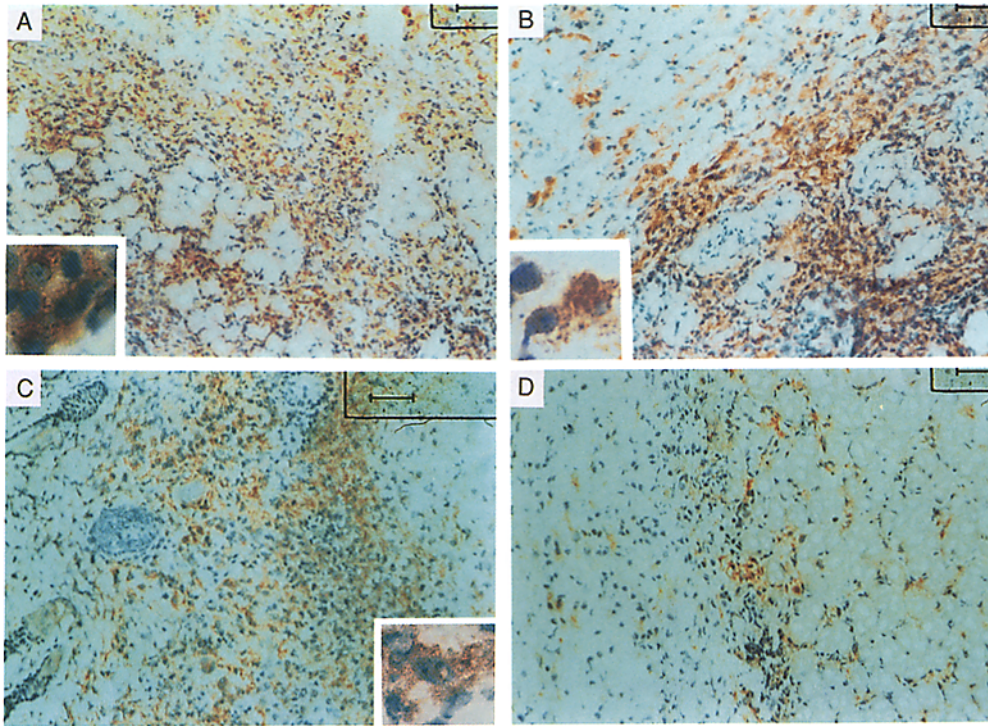
**Figure 6.** Cytokine expression in the skin of *L. major*–infected BALB/c and C57BL/6 mice. BALB/c and C57BL/6 mice were intradermally infected with *L. major* at the base of the tail. At 2, 4, 8, and 16 d after infection, the skin lesions were excised and processed for the detection of cytokines by one-color immunoperoxidase labeling. Micrographs represent sections from 8 d–infected mice. As the anti-IFN-γ and anti-IL-4 staining were indistinguishable in C57BL/6 and BALB/c lesions, the results for only one strain are shown. (*A*) BALB/c, anti-IFN-γ, ×200 (*inset* ×1,000); (*B*) C57BL/6, anti-IL-4, ×200 (*inset* ×1,000); (*C*) BALB/c, anti-TGF-β, ×200 (*inset* ×1,000); (*D*) C57BL/6, anti-TGF-β, ×200. Bars, 50 μM.

*Anti-CD4 Treatment Restores the Expression of iNOS in L. major–infected BALB/c Mice.* Susceptible BALB/c mice can be rendered resistant to *L. major* by a number of therapeutic interventions (for a review see reference 46) including systemic application of anti-CD4 before infection (47). As expected, anti-CD4–treated BALB/c mice exhibited a healing phenotype similar to that of C57BL/6 mice (Fig. 5 *A*). The clinical protection was accompanied by strikingly enhanced expression of iNOS both in the lesion (data not shown) and the LN (Fig. 5 *B*) which adds further evidence to the host-protective role of iNOS in *L. major*–infected mice.

*Inverse Expression of iNOS and TGF-β in the Lesions of Resistant and Susceptible Mice.* Next, we attempted to identify cytokines that might be responsible for the reduced tissue expression of iNOS in BALB/c mice. We chose to analyze the primary site of infection, i.e., the cutaneous lesion, which, in contrast to the draining LN, has not yet been studied for the expression of cytokines during murine cutaneous leishmaniasis (for a review see reference 46). Using immunoenzymatic labeling we found distinct infiltrates of IL-4 and IFN-γ–positive cells in *L. major*–infected skin at day 8, 12, and 16, but not at day 2 or 4 of infection (Fig. 6, *A* and *B*). The
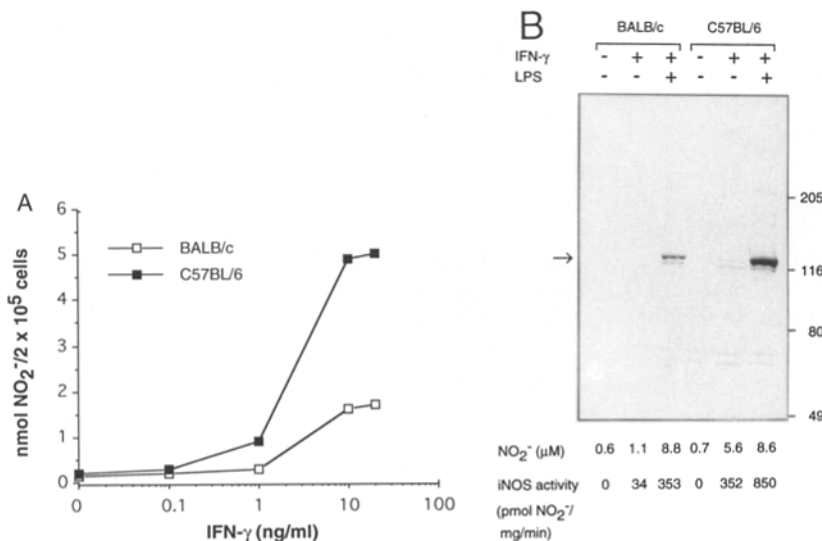


**Figure 7.** Induction of iNOS in BALB/c and C57BL/6 macrophages. Thioglycollate-elicited macrophages from BALB/c and C57BL/6 mice were cultured in medium alone or stimulated with various concentrations of IFN-γ (*A*) or IFN-γ (10 ng/ml) ± LPS (10 ng/ml) (*B*). After 48 h, accumulation of NO$_2^-$ in the culture supernatants was measured. (*B*) Total cell lysates from unstimulated or activated macrophages were processed for determination of iNOS enzyme activity, subjected to 7.5% SDS-PAGE (20 μg protein/lane), ar d immunoblotted with an iNOS-specific antiserum (18). (→) Position of the typical iNOS doublet (ca. 130 kD). One of three similar experiments.

level of expression, however, was absolutely comparable in BALB/c and C57BL/6 mice (data not shown) despite the striking differences in the amount of iNOS described above. In contrast, the lesions of BALB/c mice contained a greatly increased number of cells staining positively for TGF-$\beta$ (Fig. 6, $C$ and $D$). By the same immunohistological method, we were unable to find IL-10 in the cutaneous infiltrates. These results suggest that BALB/c mice do not lack IFN-$\gamma$ for the induction of iNOS and implicate TGF-$\beta$ as a potential downregulator of iNOS in the cutaneous lesion of BALB/c mice.

*Poor Induction of iNOS in BALB/c, but Not in C57BL/6 Macrophages after Stimulation with IFN-$\gamma$ Alone.* Previously, it was reported that BALB/c macrophages release lower amounts of NO as compared to C57BL/6 cells after stimulation with IFN-$\gamma$ plus LPS (48). As BALB/c macrophages respond poorly to LPS (49), and LPS is not a stimulus involved in the activation of macrophages during an infection with *L. major*, we investigated the expression of iNOS in macrophages from both species after activation with IFN-$\gamma$ in the absence of LPS. At optimal concentrations of IFN-$\gamma$ (10 or 20 ng/ml) accumulation of $NO_2^-$ by BALB/c macrophages was 2.9 ($\pm 0.5$)-fold lower than in respective C57BL/6 cultures (mean $\pm$ SEM of 17 experiments) (Fig. 7 $A$). Accordingly, the expression of iNOS protein and enzyme activity was strikingly reduced in BALB/c macrophages activated by IFN-$\gamma$ alone, but could be at least partially restored after costimulation with IFN-$\gamma$ and LPS (Fig. 7 $B$). It is possible that the hyporesponsiveness of BALB/c macrophages to IFN-$\gamma$ contributes to the reduced expression of iNOS in BALB/c mice in vivo.

## Discussion

Antimicrobial activity of NO in vivo was previously suggested by reports which either documented high urinary excretion of nitrate in resistant mice infected with bacteria (50, 51) or *L. major* (20), or demonstrated progressive disease in animals treated with L-NMMA (19, 20, 52–54), an inhibitor of both the constitutive and inducible type of NOS. Furthermore, by Northern blot or nonquantitative PCR analysis, iNOS mRNA was detected in tissue after the infection of mice with toxoplasma, listeria, or viruses (54–56). In this study we resorted to immunohistological techniques and competitive PCR analysis to characterize the cellular distribution of the cytokine-regulated isoform of NOS and to reliably quantitate iNOS mRNA in *L. major*-infected tissue. This combined approach provided novel evidence for an antimicrobial function of NO in vivo. First, in the skin lesions and draining LN of mice resistant to *L. major* iNOS protein was expressed earlier and in much higher amounts when compared to tissue from susceptible mice. Similarly, the peak iNOS mRNA levels in resistant mice exceeded those in nonhealing animals by a factor of at least 6–10. Second, induction of resistance in BALB/c mice via anti-CD4 treatment was paralleled by enhanced tissue expression of iNOS indistinguishable from the pattern seen in the healer strain C57BL/6. Third, in situ, no or only few parasites were detected in infiltrates of macrophages strongly positive for iNOS, whereas large

numbers of parasites were found in iNOS-negative regions. Expression of iNOS coincided locally with the presence of NADPH diaphorase activity. The appearance of NADPH diaphorase in the tissue might be due to iNOS itself (57), but could also result from other enzymes, e.g., NADPH oxidase, which is known to be upregulated in activated macrophages. In fact, coexpression of iNOS and NADPH oxidase in *L. major*-infected macrophages in vivo could be advantageous to the host as NO and reactive oxygen intermediates can lead to the generation of *trans*-peroxynitrite and finally yield the highly toxic hydroxyl-radical (58).

In vitro, many cell types exhibit iNOS activity after exposure to cytokines (3) suggesting that in vivo, widely spread expression of iNOS might follow a strong inflammatory stimulus. Studying the skin and LN of *L. major*-infected mice, we did not find universal expression of iNOS. The epidermis of the skin lesion was always negative for iNOS, and so were structurally intact follicles of the LN. After double labeling of sections from *L. major*-infected LN, macrophages could be identified as iNOS-positive cells. In contrast, B220$^+$ B and iNOS$^+$ cells were clearly separate cell populations located in distinct areas of the LN. Despite repeated attempts, we have also been unable to demonstrate expression of iNOS by Thy1$^+$ T lymphocytes, which were freshly isolated from naive or *L. major*-infected mice and (re-) stimulated in vitro (data not shown; C. Bogdan, et al., manuscript in preparation). These results do not exclude the possibility that certain T cell clones grown in vitro might release NO as reported recently (59, 60). Restricted expression of iNOS is further suggested by our competitive PCR data. Based on the crude assumption that reverse transcription and subsequent PCR amplification are equally efficient for iNOS and $\beta$-actin mRNA, there are 1–10 iNOS mRNA molecules per $10^5$ $\beta$-actin mRNA molecules in *L. major*-infected LN of resistant mice (Fig. 1 $C$). In contrast, the respective values for IL-4 or IFN-$\gamma$ mRNA are roughly 1,000-fold higher (Gessner, A., personal communication). Whether iNOS is induced in granulocytes, NK, dendritic, or Langerhans cells during the course of infection with *L. major*, is not yet known. From day 30 of infection onwards, isolated iNOS-positive cells were regularly detected in the spleen and liver, but not in the pancreas, kidney, heart, or lung of BALB/c and C57BL/6 mice (data not shown). This finding might reflect the spread of low numbers of parasites to these organs as recently observed even in resistant animals (Laskay, T., A. Diefenbach, M. Röllinghoff, and W. Solbach, manuscript in preparation). Within the time period investigated ($\leq$day 41) the limited expression of iNOS protein in spleen and liver was similar in *L. major*-infected BALB/c and C57BL/6 mice, but the BALB/c organs were loaded with parasites, presumably due to the insufficient "iNOS barrier" in the primary lesion and the draining LN (data not shown).

Two potential mechanisms for the differential regulation of iNOS in resistant and susceptible mice were identified which might act in concert. First, in vitro, the inducibility of iNOS protein and activity by IFN-$\gamma$ alone is much lower in BALB/c than in C57BL/6 macrophages. This observation extends earlier studies, where BALB/c macrophages were found to be

hyporesponsive to LPS or IFN-γ/LPS (48, 49). Second, in vivo, we noted a much more prominent expression of TGF-β in the lesions of nonhealing BALB/c when compared to resistant C57BL/6 mice. In the past, mRNA studies or restimulation experiments demonstrated that *L. major*–infected BALB/c mice maintain increased levels of IL-4 and, to a considerably lesser extent, also of IL-10 in the lymphoid tissue (23–28). TGF-β, IL-4, and IL-10 were all show to suppress the production of NO by cultured macrophages (12–15, 17, 18). Using immunohistological techniques we succeeded in detecting cytokines in the dermal infiltrates after *L. major* infection; this has not yet been reported. Data presented here suggest that IL-4, which was found at comparable levels in the infected skin of BALB/c and C57BL/6 mice, is not responsible for the downregulation of iNOS in the cutaneous lesions of BALB/c mice. Furthermore, BALB/c mice do not lack IFN-γ at the primary site of infection. In contrast, the different amount of iNOS protein in the lesions of susceptible and resistant mice correlated well with high or low level expression of TGF-β, respectively. Our study provides evidence that TGF-β downregulates iNOS in vivo, a function that might underlie the previously reported disease-promoting effect of TGF-β (34). In vitro, TGF-β suppresses iNOS protein, but not iNOS mRNA if added to already activated macrophages (18). This unique function of TGF-β might explain the strikingly different expression of iNOS protein in the skin of BALB/c and C57BL/6 mice at day 4–12 of infection (Fig. 2), when the levels of iNOS mRNA were still similar in the lesions of both strains (Fig. 1 C). It should be noted that the situation might be different in the LN where we could not reliably document the expression of TGF-β. Instead, we found persistent levels of IL-4 mRNA in infected BALB/c, but not in C57BL/6 mice, whereas the expression of IFN-γ mRNA was comparable in the LN of both strains

of mice (data not shown). This finding confirms a recent report by Reiner et al. (28) and leaves the possibility that IL-4 (and perhaps also IL-10) contributes to the reduction of iNOS in the LN of *L. major*–infected BALB/c mice as described in our present study.

During the kinetic analysis of *L. major*–infected mice we found significant amounts of iNOS expressed in the skin and draining LN of resistant mice even after the cutaneous lesions were clinically almost completely healed (Figs. 1 and 3). Our preliminary data suggest that iNOS persists in the tissue of long-term infected resistant mice along with very small numbers of parasites (Bogdan, C., S. Stenger, H. Thüring, and M. Röllinghoff, manuscript in preparation). Live parasites have repeatedly been isolated from cured mice (61–63) and might represent a permanent signal for the local induction of iNOS. This could be part of a finely tuned host–parasite relationship, where the persistence of *Leishmania* is required for the maintenance of host immunity while simultaneous expression of iNOS prevents uncontrolled parasite replication and reduces the level of T cell activity (64–67).

In summary, the experiments presented here provide novel information about the regulation of iNOS in vivo. First, the amount of iNOS in the skin lesion and the lymphoid tissue of *L. major*–infected mice correlates inversely with the clinical course of disease. Second, macrophages are the predominant if not the only cell population devoted to the production of NO in the LN. Third, in situ areas rich in iNOS are devoid of parasites. Fourth, increased levels of TGF-β in the tissue (and perhaps also hyporesponsiveness to IFN-γ) might account for the reduced expression of iNOS in susceptible mice. Our current studies are focussed on the regulation of TGF-β in order to understand its differential appearance in resistant and susceptible mice.

## References

1. Stuehr, D., and M.A. Marletta. 1985. Mammalian nitrite biosynthesis: mouse macrophages produce nitrite and nitrate in response to *Escherichia coli* lipopolysaccharide. *Proc. Natl. Acad. Sci. USA.* 82:7738.

2. Stuehr, D.J., and O.W. Griffith. 1992. Mammalian nitric oxide synthases. *Adv. Enz. Rel. Areas Mol. Biol.* 65:287.

3. Nathan, C. 1992. Nitric oxide as a secretory product of mammalian cells. *FASEB (Fed. Am. Soc. Exp. Biol.) J.* 6:3051.

4. Marletta, M.A. 1993. Nitric oxide synthase structure and mechanism. *J. Biol. Chem.* 268:12231.

5. Moncada, S., and A. Higgs. 1993. The L-arginine-nitric oxide pathway. *N. Engl. J. Med.* 329:2002.

6. Nathan, C., and J.B. Hibbs, Jr. 1991. Role of nitric oxide synthesis in macrophage antimicrobial activity. *Curr. Opin. Immunol.* 3:65.

7. Green, S.J., and C.A. Nacy. 1993. Antimicrobial and immunopathologic effects of cytokine-induced nitric oxide synthesis. *Curr. Opin. Infect. Dis.* 6:384.

8. Karupiah, G., Q.-w. Xie, M.L. Buller, C. Nathan, C. Duarte, and J.D. MacMicking. 1993. Inhibition of viral replication by interferon-γ-induced nitric oxide synthase. *Science (Wash. DC).* 261:1445.

9. Bogdan, C., Y. Vodovotz, Q.-w. Xie, C. Nathan, and M. Röllinghoff. 1994. Regulation of inducible nitric oxide synthase in macrophages by cytokines and microbial products. *In* Immunotherapy of Infections. N. Masihi, editor. Marcel Dekker, Inc., New York. 37–54.

10. Bastian, N.R., and J.B. Hibbs, Jr. 1994. Assembly and regulation of NADPH oxidase and nitric oxide synthase. *Curr. Opin. Immunol.* 6:131.

11. Ding, A.H., C.F. Nathan, and D.J. Stuehr. 1988. Release of reactive nitrogen intermediates and reactive oxygen intermediates from mouse peritoneal macrophages. Comparison of activating cytokines and evidence for independent production. *J. Immunol.* 141:2407.

12. Liew, F.Y., Y. Li, A. Severn, S. Millott, J. Schmidt, M. Salter, and S. Moncada. 1991. A possible novel pathway of regulation by murine T helper type-2 (Th2) cells of a Th1 cell activity via the modulation of the induction of nitric oxide synthase in macrophages. *Eur. J. Immunol.* 21:2489.

13. Bogdan, C., Y. Vodovotz, J. Paik, Q.-w. Xie, and C. Nathan. 1994. Mechanism of suppression of nitric oxide synthase expression by interleukin 4 in primary mouse macrophages. *J. Leukocyte Biol.* 55:227.

14. Bogdan, C., Y. Vodovotz, and C. Nathan. 1991. Macrophage deactivation by interleukin-10. *J. Exp. Med.* 174:1549.

15. Gazzinelli, R.T., I.P. Oswald, S.L. James, and A. Sher. 1992. IL-10 inhibits parasite killing and nitrogen oxide production by IFN-γ activated macrophages. *J. Immunol.* 148:1792.

16. Doherty, T.M., R. Kastelein, S. Menon, S. Andrade, and R.L. Coffman. 1993. Modulation of murine macrophage function by IL-13. *J. Immunol.* 151:7151.

17. Ding, A., C.F. Nathan, J. Graycar, R. Derynck, D.J. Stuehr, and S. Srimal. 1990. Macrophage deactivating factor and transforming growth factors-β1, -β2, and -β3 inhibit induction of macrophage nitrogen oxide synthesis by IFN-γ. *J. Immunol.* 145:940.

18. Vodovotz, Y., C. Bogdan, J. Paik, Q.-w. Xie, and C. Nathan. 1993. Mechanisms of suppression of macrophage nitric oxide release by transforming growth factor β. *J. Exp. Med.* 178:605.

19. Liew, F.Y., S. Millott, C. Parkinson, R.M.J. Palmer, and S. Moncada. 1990. Macrophage killing of *Leishmania* parasite *in vivo* is mediated by nitric oxide from L-arginine. *J. Immunol.* 144:4794.

20. Evans, T.G., L. Thai, D.L. Granger, and J.B. Hibbs, Jr. 1993. Effect of in vivo inhibition of nitric oxide production in murine leishmaniasis. *J. Immunol.* 151:907.

21. Green, S.J., M.S. Meltzer, J.B. Hibbs, Jr., and C.A. Nacy. 1990. Activated macrophages destroy intracellular *Leishmania major* amastigotes by an L-arginine–dependent killing mechanism. *J. Immunol.* 144:278.

22. Liew, F.Y., Y. Li, and S. Millott. 1990. Tumor necrosis factor-α synergizes with IFN-γ in mediating killing of Leishmania major through the induction of nitric oxide. *J. Immunol.* 145:4306.

23. Heinzel, F.P., M.D. Sadick, B.J. Holaday, R.L. Coffman, and R.M. Locksley. 1989. Reciprocal expression of interferon-γ or interleukin 4 during the resolution or progression of murine leishmaniasis. Evidence for expansion of distinct helper T cell subsets. *J. Exp. Med.* 169:59.

24. Heinzel, F.P., M.D. Sadick, S.S. Mutha, and R.M. Locksley. 1991. Production of interferon-γ, interleukin 2, interleukin 4 and interleukin 10 by CD4+ lymphocytes in vivo during healing and progressive murine leishmaniasis. *Proc. Natl. Acad. Sci. USA.* 88:7011.

25. Boom, W.H., L. Liebster, A.K. Abbas, and R.G. Titus. 1990. Patterns of cytokine secretion in murine leishmaniasis: correlation with disease progression or resolution. *Infect. Immun.* 58:3863.

26. Moll, H., and M. Röllinghoff. 1990. Resistance to murine cutaneous leishmaniasis is mediated by Th1 cells, but disease-promoting CD4+ cells are different from Th2 cells. *Eur. J. Immunol.* 20:2067.

27. Morris, L., A.B. Troutt, K.S. McLeod, A. Kelso, E. Handman, and T. Aebischer. 1993. Interleukin-4, but not interferon production correlates with the severity of murine cutaneous leishmaniasis. *Infect. Immun.* 61:3459.

28. Reiner, S.L., S. Zheng, Z.-E. Wang, L. Stowring, and R.M. Locksley. 1994. Leishmania promastigotes evade interleukin 12 (IL-12) induction by macrophages and stimulate a broad range of cytokines from CD4+ T cells during initiation of infection. *J. Exp. Med.* 179:447.

29. Scott, P., P. Natovitz, R.L. Coffman, E. Pearce, and A. Sher. 1988. Immunoregulation of cutaneous leishmaniasis. T cell lines that transfer protective immunity or exacerbation belong to different T helper subsets and respond to distinct parasite antigens. *J. Exp. Med.* 168:1675.

30. Belosevic, M., D.S. Finbloom, P.H. van der Meide, M.V. Slayter, and C.A. Nacy. 1989. Administration of monoclonal anti-IFN-γ antibodies in vivo abrogates natural resistance of C3H/HeN mice to interferon with *Leishmania major*. *J. Immunol.* 143:266.

31. Sadick, M.D., F.P. Heinzel, B.J. Holaday, R.T. Pu, R.S. Dawkins, and R.M. Locksley. 1990. Cure of murine leishmaniasis with anti-interleukin 4 monoclonal antibody. Evidence for a T cell–dependent, interferon-γ–independent mechanism. *J. Exp. Med.* 171:115.

32. Scott, P. 1991. IFN-γ modulates the early development of Th1 and Th2 responses in a murine model of cutaneous leishmaniasis. *J. Immunol.* 147:3149.

33. Powrie, F., S. Menon, and R.L. Coffman. 1993. Interleukin-4 and interleukin-10 synergize to inhibit cell-mediated immunity *in vivo*. *Eur. J. Immunol.* 23:3043.

34. Barral-Netto, M., A. Barral, C.E. Brownell, Y.A.W. Skeiky, L.R. Ellingsworth, D.R. Twardzik, and S.G. Reed. 1992. Transforming growth factor-β in leishmanial infection: a parasite escape mechanism. *Science (Wash. DC).* 257:545.

35. Solbach, W., K. Forberg, and M. Röllinghoff. 1986. Effect of T-lymphocyte suppression on the parasite burden in *Leishmania major*-infected, genetically susceptible BALB/c mice. *Infect. Immun.* 54:909.

36. Blank, C., H. Fuchs, K. Rappersberger, M. Röllinghoff, and H. Moll. 1993. Parasitism of epidermal Langerhans cells in experimental cutaneous Leishmaniasis with *Leishmania major*. *J. Infect. Dis.* 167:418.

37. Sacks, D., S. Hieny, and A. Sher. 1985. The identification of cell surface carbohydrate and antigenic changes between noninfective and infective developmental stages of *Leishmania major* promastigotes. *J. Immunol.* 135:564.

38. Xie, Q.-w., H.J. Cho, J. Calaycay, R.A. Mumford, K.M. Swiderek, T.D. Lee, A. Ding, T. Troso, and C. Nathan. 1992. Cloning and characterization of inducible nitric oxide synthase from mouse macrophages. *Science (Wash. DC).* 256:225.

39. Chomczynski, P., and N. Sacchi. 1987. Single-step method of RNA isolation by acid guanidinium thiocyanate-phenol-chloroform extraction. *Anal. Biochem.* 162:156.

40. Gilliland, G., S. Perrin, K. Blanchard, and H.F. Bunn. 1990. Analysis of cytokine mRNA and DNA: detection and quantitation by competitive polymerase chain reaction. *Proc. Natl. Acad. Sci. USA.* 87:2725.

41. Tokunaga, K., H. Taniguchi, K. Yoda, M. Shimizu, and S. Sakiyama. 1986. Nucleotide sequence of a full-length cDNA for mouse cytoskeletal β-actin mRNA. *Nucleic Acid Res.* 14:2829.

42. Maniatis, T., E.F. Fritsch, and J. Sambrook. 1989. Molecular Cloning: A Laboratory Manual. Cold Spring Harbor Laboratory, Cold Spring Harbor, NY. 9.31–9.62.

43. Gillitzer, R., and H. Moll. 1993. Simultaneous demonstration of two antigens with immunogold-silver staining and immunoenzymatic labeling. *J. Histotechnol.* 16:223.

44. Hope, B.T., G.J. Michael, K.M. Knigge, and S.R. Vincent. 1991. Neuronal NADPH diaphorase is a nitric oxide synthase. *Proc. Natl. Acad. Sci. USA.* 88:2811.

45. Kraal, G., M. Rep, and M. Janse. 1987. Macrophages in T and B cell compartments and other tissue macrophages recognized by monoclonal antibody MOMA-2. *Scand. J. Immunol.* 26:6553.

46. Bogdan, C., A. Gessner, and M. Röllinghoff. 1993. Cytokines in leishmaniasis: a complex network of stimulatory and inhibitory interactions. *Immunobiology.* 189:356.

47. Titus, R.G., R. Ceredig, J.C. Cerottini, and J.A. Louis. 1985. Therapeutic effect of anti-L3T4a monoclonal antibody GK 1.5 on cutaneous leishmaniasis in genetically susceptible BALB/c mice. *J. Immunol.* 135:2108.

48. Liew, F.Y., Y. Li, D. Moss, C. Parkinson, M.V. Rogers, and S. Moncada. 1991. Resistance to *Leishmaniasis major* infection correlates with the induction of nitric oxide synthase in murine macrophages. *Eur. J. Immunol.* 21:3009.

49. Oswald, I.P., S. Afroun, D. Bray, J.-F. Petit, and G. Lemaire. 1992. Low response of BALB/c macrophages to priming and activating signals. *J. Leukocyte Biol.* 52:315.

50. Granger, D., J.B. Hibbs, Jr., and L.M. Broadnax. 1991. Urinary nitrate excretion in relation to murine macrophage activation. Influence of dietary L-arginine and oral N-monomethyl-L-arginine. *J. Immunol.* 146:1294.

51. Green, S.J., C.A. Nacy, R.D. Schreiber, D.L. Granger, R.M. Crawford, M.S. Meltzer, and A.H. Fortier. 1993. Neutralization of gamma interferon and tumor necrosis factor alpha blocks in vivo synthesis of nitrogen oxides from L-arginine and protection against *Francisella tularensis* infection in *Mycobacterium bovis* BCG–treated mice. *Infect. Immun.* 61:689.

52. Beckerman, K.P., H.W. Rogers, J.A. Corbett, R.D. Schreiber, M.L. McDaniel, and E.R. Unanue. 1993. Release of nitric oxide during the T-cell–independent pathway of macrophage activation. *J. Immunol.* 150:888.

53. Nüssler, A.K., L. Rénia, V. Pasquetto, F. Miltgren, H. Ma-

tile, and D. Mazier. 1993. In vivo induction of the nitric oxide pathway in hepatocytes after injection with irradiated malaria sporozoites, malaria blood parasites or adjuvants. *Eur. J. Immunol.* 23:882.

54. Boockvar, K.S., D.S. Granger, R.M. Poston, M. Maybodi, M.K. Washington, J.B. Hibbs, and R.L. Kurlander. 1994. Nitric oxide produced during murine listeriosis is protective. *Infect. Immun.* 62:1089.

55. Gazzinelli, R.T., I. Eltoum, T.A. Wynn, and A. Sher. 1993. Acute cerebral toxoplasmosis is induced by in vivo neutralization of TNF-α and correlates with the down-regulated expression of inducible nitric oxide synthase and other markers of macrophage activation. *J. Immunol.* 151:3672.

56. Koprowski, H., Y.M. Zheng, E. Heber-Katz, N. Fraser, L. Rorke, Z.F. Fu, C. Hanlon, and B. Dietzschold. 1993. In vivo expression of inducible nitric oxide synthase in experimentally induced neurologic diseases. *Proc. Natl. Acad. Sci. USA.* 90:3024.

57. Tracey, W.R., M. Nakane, J.S. Pollock, and U. Förstermann. 1993. Nitric oxide synthases in neuronal cells, macrophages, and endothelium are NADPH diaphorases, but represent only a fraction of total cellular NADPH diaphorase activity. *Biochem. Biophys. Res. Commun.* 195:1035.

58. Beckman, J.S., T.W. Beckman, J. Chen, P.A. Marshall, and B.A. Freeman. 1990. Apparent hydroxyl radical production by peroxynitrite: implications for endothelial injury from nitric oxide and superoxide. *Proc. Natl. Acad. Sci. USA.* 87:1620.

59. Kirk, S.J., M.C. Regan, and A. Barbul. 1990. Cloned murine T lymphocytes synthesize a molecule with the biological characteristics of nitric oxide. *Biochem. Biophys. Res. Commun.* 173:660.

60. Taylor-Robinson, A.W., F.Y. Liew, A. Severn, D. Xu, S.J. McScorley, P. Garside, J. Padron and R.S. Phillips. 1994. Regulation of the immune response by nitric oxide differentially produced by T helper type 1 and T helper type 2 cells. *Eur. J. Immunol.* 24:980.

61. Hill, J.O., R.J. North, and F.M. Collins. 1983. Advantages of measuring changes in the number of viable parasites in murine models of experimental cutaneous leishmaniasis. *Infect. Immun.* 39:1087.

62. Titus, R.G., M. Marchand, T. Boon, and J.A. Louis. 1985. A limiting dilution assay for quantifying *Leishmania major* in tissues of infected mice. *Parasite Immunol. (Oxf).* 7:545.

63. Aebischer, T., S.F. Moody, and E. Handman. 1993. Persistence of virulent *Leishmania major* in murine cutaneous leishmaniasis: a possible hazard for the host. *Infect. Immun.* 61:220.

64. Albina, J.E., J.A. Abate, and W.L. Henry, Jr. 1991. Nitric oxide production is required for murine resident peritoneal macrophages to suppress mitogen-stimulated T cell proliferation. Role of IFN-γ in the induction of the nitric oxide–synthesizing pathway. *J. Immunol.* 147:144.

65. Gregory, S.H., E.J. Wing, R.A. Hoffman, and R.L. Simmons. 1993. Reactive nitrogen intermediates suppress the primary immunologic response to *Listeria. J. Immunol.* 150:2901.

66. Sternberg, J., and F. McGuigan. 1992. Nitric oxide mediates suppression of T cell responses in murine *Trypanosoma brucei* infection. *Eur. J. Immunol.* 22:2741.

67. Stefani, M.M.A., I. Müller, and J. Louis. 1994. *Leishmania major*–specific CD8+ T cells are inducers and targets of nitric oxide produced by parasitized macrophages. *Eur. J. Immunol.* 24:746.